# Non-retracing orbits in Andreev billiards

Florian Libisch,* Stefan Rotter, and Joachim Burgdörfer
*Institute for Theoretical Physics, Vienna University of Technology, Wiedner Hauptstraße 8-10/136, A-1040 Vienna, Austria, EU*
(Received 26 September 2005; revised manuscript received 23 November 2005; published 24 January 2006)

The validity of the retracing approximation in the semiclassical quantization of Andreev billiards is investigated. The exact energy spectrum and the eigenstates of normal-conducting, ballistic quantum dots in contact with a superconductor are calculated by solving the Bogoliubov-de Gennes equation and compared with the semiclassical Bohr-Sommerfeld quantization for periodic orbits which result from Andreev reflections. We find deviations that are due to the assumption of exact retracing electron-hole orbits rather than the semiclassical approximation, as a concurrently performed Einstein-Brillouin-Keller quantization demonstrates. We identify three different mechanisms producing non-retracing orbits which are directly identified through differences between electron and hole wave functions.

DOI: 10.1103/PhysRevB.73.045324 PACS number(s): 73.23.Ad, 74.45.+c, 03.65.Sq, 73.63.Kv

## I. INTRODUCTION

The dynamics of hybrid systems consisting of a normal-conducting (N) quantum dot and a superconducting (S) wave guide have recently raised much experimental[1–3] and theoretical[4–12] interest. This is due to the unusual and sometimes counterintuitive properties of the interface of normal- and superconducting regions. An electron moving inside the N region will be coherently scattered into a hole upon contact with the superconductor [see Fig. 1(a)].[13] This phenomenon is commonly referred to as Andreev reflection.[14] In the frequently used and remarkably successful semiclassical Bohr-Sommerfeld (BS) method[15–17] it is assumed that the Andreev reflection is perfect, i.e., that the path of the back-scattered hole will exactly trace that of the incoming electron ($\vec{v}_e=-\vec{v}_h$) [see Fig. 1(b)]. The consequences of this assumption are profound: all trajectories emanating from the SN interface are strictly periodic. The classical dynamics of the combined SN system become entirely regular, even and in particular when the normal-conducting cavity would feature hard chaos.[18] Unlike chaotic or integrable systems, periodic orbits are no longer isolated but form continuous manifolds that dominate the classical phase space and, in turn, the density of states (DOS).[19–21] The BS approach[15,16,22] to the DOS of an Andreev billiard relies on three assumptions: exact retracing of electron-hole trajectories (referred to as assumption A1 in the following), the absence of any (quasi-)periodic orbits other than the ones caused by Andreev reflection (assumption A2), and the applicability of semiclassical approximations (assumption A3), i.e., $\lambda_D \ll \sqrt{A}$, where $\lambda_D$ is the de Broglie wavelength and $A$ is the area of the N billiard.

The BS approximation has been found to be surprisingly accurate,[15,22] even in the presence of a magnetic field[16] or a soft wall potential.[23] However, some difficulties have emerged: for example, the excitation gap in the DOS for billiards with a chaotic N cavity cannot be properly accounted for.[24–26] A direct inspection of the electron- and hole-components of the wave functions[23,27] revealed markedly different patterns, clearly signaling a breakdown of the retracing approximation.

In the present communication, we investigate the role of non-retracing orbits in Andreev billiards. Non-retracing electron-hole orbits leave their mark on the Andreev wave functions which we determine by solving the Bogoliubov-de Gennes equation with the help of the modular recursive Green's function method (MRGM).[28,29] We find that Andreev states which correspond to non-retracing orbits break the close correspondence between the electron and hole wave function patterns. The analysis of the eigenstates allows us to check the merits and limitations of the BS approximation against the exact quantum mechanical approach. We identify different sources for the breakdown and explore separately each of the assumptions A1 to A3 listed above.

This paper is organized as follows. In Sec. II the method for solving the quantum mechanical eigenvalue problem as well as the Bohr-Sommerfeld approach to Andreev billiards is briefly reviewed. In Sec. III we identify different mechanisms leading to non-retracing orbits in Andreev billiards. The paper concludes with a short summary in Sec. IV.

## II. MODEL SYSTEM

We consider as a model system a rectangular normal-conducting cavity of width $D$, length $L$, and area $A=LD$, which is attached to a half-infinite lead of width $W$ [see Fig. 1(a)]. For technical reasons we focus on an N cavity that features classically regular motion. Since within the framework of perfect Andreev reflections combined SN-Andreev systems become regular and, in fact, periodic irrespective of the underlying regular or chaotic dynamics of the N cavity, we expect many of our results to be valid for arbitrary N cavities. As we consider only one superconducting lead, we choose the gap parameter $\Delta$ to be real. The superconducting coherence length ($\xi$) is assumed to be small compared to the linear dimension of the rectangular cavity ($\sim\sqrt{A}$). Under that assumption we may use a step function model[7] at the SN interface, $\Delta=|\Delta_0|\Theta(x_{NS}-x)$. This SN interface, which is located at $x_{NS}=0$, is assumed to be ideal, meaning that there is no tunnel barrier and no mismatch between Fermi energies and effective masses in the N and S regions. An exact treatment of the Bogoliubov-de Gennes equation reveals that this results in a probability for Andreev reflection close to unity (up to corrections of the order $\Delta^2/E_F^2$) in the energy range we

 

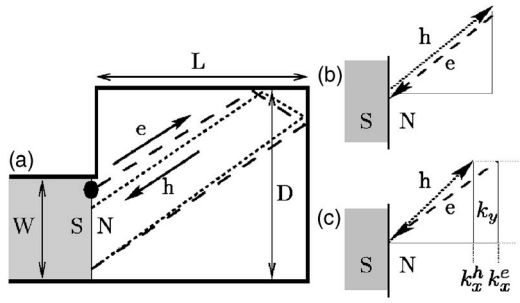


FIG. 1. (a) Andreev billiard with a rectangular normal-conducting (N) region. The superconducting (S) lead is assumed to be half-infinite (shaded area). The dashed and dotted lines depict an "almost retracing" electron-hole orbit created by Andreev reflection at the SN interface. For better visibility the starting point of the orbit is marked by a dot. (b) Perfect Andreev reflection, i.e., $\theta_e = \theta_h$. (c) Imperfect Andreev reflection, $\theta_e \neq \theta_h$, $k_y^e = k_y^h$.

consider, $0 \leqslant \varepsilon \leqslant \Delta = 0.02 E_F$.[11,13] Furthermore, the phase coherence length of the scattering process is assumed to be infinitely long, resulting in fully ballistic dynamics.

### A. Quantum mechanical solution

We describe the S-N hybrid system by the Bogoliubov-de Gennes (BdG) equation[30]

$$\begin{pmatrix} H_0 & \Delta \\ \Delta^* & -H_0^* \end{pmatrix} \begin{pmatrix} u(\mathbf{x}) \\ v(\mathbf{x}) \end{pmatrix} = \varepsilon \begin{pmatrix} u(\mathbf{x}) \\ v(\mathbf{x}) \end{pmatrix}. \tag{1}$$

$H_0 = p^2/(2m_{\text{eff}}) + V(r) - E_F$ is the single-particle Hamiltonian. The electron (hole) quasi-particle wave functions are denoted by $u$ ($v$); $\varepsilon$ is the excitation energy of the electron (hole) above (below) the Fermi energy $E_F$. Throughout this publication we consider only bound Andreev states for which the solutions of (1) in the superconducting region are exponentially decaying. To identify the bound Andreev states, we use a wave function matching technique[15] in combination with the modular recursive Green's function method[28,29] as outlined in Ref. 23.

Note that the above procedure is exact in the sense that it does not rely on the usual Andreev appoximation, namely $\Delta \ll E_F$, and the assumption of approximately perpendicular angles of incidence on the SN interface.[13,14] This feature will be important when we consider the effect of imperfect Andreev reflections on the quantum and semiclassical spectra.

### B. Semiclassical analysis

The intuitive picture of ideal Andreev reflections [Fig. 1(b)] lends itself to a semiclassical description and, more specifically, to a periodic-orbit quantization. An electron approaches the SN interface with wave number

$$k_e = \sqrt{2(E_F + \varepsilon)} \tag{2}$$

and angle $\theta_e$ relative to the interface normal. The hole leaves the interface with wave number

$$k_h = \sqrt{2(E_F - \varepsilon)} \tag{3}$$

and a corresponding angle $\theta_h$. Since the component along the interface is exactly conserved because of translational invariance, $k_{e,y} = k_{h,y}$ (or $v_{e,y} = -v_{h,y}$), the components normal to the interface will be, in general, different, $k_{e,x} \neq k_{h,x}$, leading to imperfect retracing [Fig. 1(c)]. Only in the limit $\varepsilon \to 0$ (or $\varepsilon/E_F \to 0$) does perfect Andreev reflection $k_{e,x} = k_{h,x}$ (or $v_{e,x} = -v_{h,x}$) ensue. The retracing approximation consists now of the assumption A1 of perfect reflection, $v_{e,x} = -v_{h,x}$, for all $\varepsilon$ in the interval $0 \leqslant \varepsilon \leqslant \Delta$. The validity and breakdown of this assumption will be explored in the following.

Under assumption A1 all trajectories emanating from the SN interface are strictly periodic. For N cavities featuring hard chaos, every trajectory will eventually hit the SN interface, thus yielding a globally periodic system. For N cavities with mixed or regular dynamics, certain regions of the phase space may remain decoupled from the interface and thus may feature both continuous manifolds of strictly periodic orbits and islands with quasi-periodic motion. Neglecting the latter contribution to the DOS implies assumption A2.

The BS quantization of the continuum of perfectly periodic orbits visiting the SN interface yields for the action $S$ of periodic orbits created by pairs of electron-hole trajectories (with wavenumbers $k_e$, $k_h$),[16]

$$S = l(k_e - k_h) = 2\pi n + 2 \arccos(\varepsilon/\Delta). \tag{4}$$

The variable $l$ stands for the length of an arbitrary path connecting one point at the SN interface with another. The quantum number $n = 0, 1, 2, \ldots$ accounts for the quantized difference in action between the electron and the hole part of the periodic orbit. The second term on the right-hand side of Eq. (4), $\arccos(\varepsilon/\Delta)$, is the Maslov index[31] for one reflection at the SN interface. Including this energy-dependent phase shift at the point of Andreev reflection extends[15] the accuracy of the BS description to energy ranges $0 \leqslant \varepsilon \leqslant \Delta$. An even more accurate semiclassical description of the Andreev reflection process will be discussed in a subsequent publication.[32]

The semiclassical BS approximation for the state counting function can then be written as[16]

$$N_{BS} = M \sum_{n=0}^{\infty} \int_{l_n(\varepsilon)}^{\infty} P(l) dl, \tag{5}$$

where $l_n(\varepsilon)$ is defined by

$$l_n(\varepsilon) = \left[ n\pi + \arccos\left(\frac{\varepsilon}{\Delta}\right) \right] \frac{k_F}{\varepsilon}. \tag{6}$$

The geometry of the cavity enters via the classical path length distribution $P(l)$. The quantity $P(l)dl$ is the classical probability that an electron entering the N region at the SN interface returns to the interface after a path length in the interval $[l, l+dl]$.

In the special case that the Andreev system becomes separable, in particular for the geometry $W = D$ [see the inset in Fig. 2(a), and Fig. 4(a)], an alternative semiclassical approximation, the Einstein-Brillouin-Keller (EBK) quantization, becomes applicable. This alternative is of particular interest as it only relies on assumption A3, but does not involve the

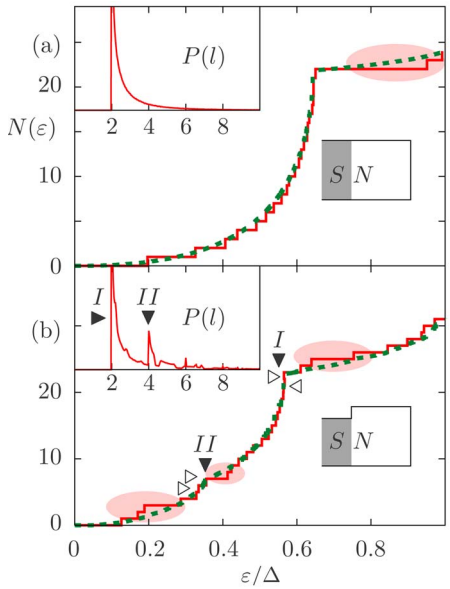


FIG. 2. (Color online) The quantum mechanical state counting function $N_{\mathrm{QM}}(\varepsilon)$ (solid red staircase) and its semiclassical BS estimate $N_{\mathrm{BS}}(\varepsilon)$ (dashed green line) for two quadratic cavities with different lead widths as shown in the insets [$k_{\mathrm{F}}=20.5\pi/W$, $W=L$(a), $0.8L$(b)]. The top left insets show the classical path length distribution in units of the cavity length $L$. Solid triangles mark pronounced cusps in $N(\varepsilon)$ and their classical origin. The quantum number $n$ [Eq. (4)] increases from 0 to 1 at the cusp marked $I$. Open triangles mark the energy positions of states whose wave functions are displayed in Fig. 3. Shading marks the regions where the BS approximation begins to deviate from quantum results.

additional assumptions A1 and A2, thus allowing to disentangle the validity of the semiclassical approximation from that of the retracing approximation. For an EBK quantization of the cavity with $W=D$ the separability yields two quantization conditions, the first one of which pertains to the motion in $x$ direction [compare with Eq. (4)],

$$\oint_{\mathcal{C}_x} k_x^{e,h}\mathrm{d}x = 2L(k_x^e - k_x^h) = 2\left[n\pi + \arccos\left(\frac{\varepsilon}{\Delta}\right)\right]. \tag{7}$$

The second quantization condition in $y$ direction reads

$$\oint_{\mathcal{C}_y} k_y \mathrm{d}y = 2k_y D = 2m\pi. \tag{8}$$

The contour $\mathcal{C}_x$ ($\mathcal{C}_y$) stands for a path along a horizontal (vertical) line in the normal conducting billiard. Introducing the short hand notation $k_x^m(\pm\varepsilon)=k_m^{\pm}$ with

$$k_m^{\pm} = \sqrt{2(E_{\mathrm{F}} \pm \varepsilon) + \left(\frac{m\pi}{W}\right)^2}, \tag{9}$$

the quantization condition for $x$ [Eq. (7)] reads

$$\left[n\pi + \arccos\left(\frac{\varepsilon}{\Delta}\right)\right] = L(k_m^+ - k_m^-). \tag{10}$$

This is a transcendental equation in $\varepsilon(n,m)$, which allows us to calculate individual energy levels in a cavity with $W=D$ semiclassically. Note that in contrast to this EBK result, the BS approach yields only an approximation to the smoothed state counting function $N(\varepsilon)$. We therefore transform the EBK results for $\varepsilon(n,m)$ into a state counting function

$$N_{EBK} = \int_0^{\varepsilon} d\varepsilon' \sum_{m,n} \delta[\varepsilon' - \varepsilon(n,m)] \tag{11}$$

and compare both semiclassical approximations with the quantum results. EBK quantization of Andreev billiards can be viewed as the analog to the adiabatic quantization of smooth soft-wall chaotic billiards, for completely integrable systems.[33,34] As the EBK quantization invokes quasi-periodic rather than periodic motion no assumption of retracing is involved.

## III. VALIDITY OF THE RETRACING APPROXIMATION

We will now explore the validity and breakdown of the retracing approximation and the resulting BS quantization by considering rectangular cavities (Fig. 4) with different ratios $D/W$ and $D/L$. With this parameter space at our disposal we can probe and disentangle the validity of assumptions A1 to A3.

### A. Quadratic $N$ cavity

We consider first the quadratic cavity with $D=L$. Here two cases arise: for $D/W=1$, the Andreev billiard becomes separable while for $D/W>1$ the Andreev system is nonseparable even though the $N$ cavity itself is separable. In the latter case the SN boundary condition breaks the separability. The location of the placement of the SN interface for $D/W>1$ provides an additional degree of freedom for our investigation to be exploited below. A comparison between the BS approximation and the exact quantum mechanical calculation for the counting function $N(\varepsilon)$ is shown in Fig. 2. Overall, for $D/W=1$ (a) and $D/W=1.25$ (b), the BS approximation performs quite well. In particular, it reproduces and intuitively explains the cusps seen in $N(\varepsilon)$. They are due to the sharp peaks in the pathlength spectrum (see inset). The position of the cusps is predicted very accurately by the BS approximation with an error well below the mean level spacing of $0.09\Delta$.

Assuming the validity of the retracing approximation, the semiclassical quantization condition [Eq. (6)] allows us to map every excitation energy $\varepsilon$ onto a path length $l_n$ of a periodic Andreev orbit. Consider, e.g., the energy at the cusp marked $I$ in Fig. 2(b) that corresponds to a path length $l_0=2L$, which is the length of the shortest classical Andreev-reflected orbit of the system [see $P(l)$ in the inset of Fig. 2(b)]: The electron leaves perpendicular to the SN interface, is reflected at the opposing wall, and returns to the SN interface. Quantum mechanical wave functions evaluated at the cusp energy indeed feature a pronounced enhancement along the orbit "bundle"[35] with length $l=2L$ [see Fig. 3(b)]. Wave functions with neighboring energy values below the cusp feature additional nodes in transverse direction [see Fig. 3(a)]. Note that also eigenstates near the cusp marked $II$ in Figs. 3(c) and 3(d) correspond very nicely to the path

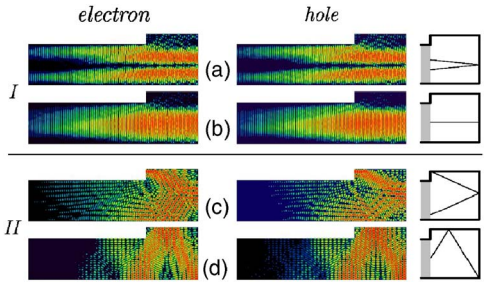


FIG. 3. (Color online) (a)–(d) show the electron and hole wave functions $|u(\mathbf{x})|^2$ and $|v(\mathbf{x})|^2$ at values of $\varepsilon$ indicated by open triangles in Fig. 2(b): $\varepsilon/\Delta$ is (a) 0.565, (b) 0.566, (c) 0.33, and (d) 0.355. The corresponding classical orbits are indicated on the right.

bundles of the expected length. Consistent with the good agreement of the BS quantization with the quantum calculations, the electron and hole wave function densities agree very well with each other. To the extent that bundles of classical trajectories cause the density enhancement in the wave function, and bundles of hole- and particle-orbits agree with each other, this is to be expected. Conversely, a hallmark of the breakdown of retracing are distinct density ditributions in the particle ($u$) and hole ($v$) wave functions, as has been recently observed.[23,27] Looking more closely, we find discrepancies between the exact quantum mechanical calculations for $N_{\mathrm{QM}}(\varepsilon)$ and its semiclassical counterpart $N_{BS}(\varepsilon)$, which are indicated by the shaded areas in Figs. 2(a) and 2(b). For the two systems considered in Fig. 2 we note that the mismatch between the quantum and the semiclassical results is located at rather well-defined values of the excitation energy $\varepsilon$. The mismatch tends to occur at values of $\varepsilon$ just *above* a cusp.

Since pathlength and energy at fixed quantum number $n$ are inversely proportional to each other [Eq. (6)] the energies *above* the cusp which is associated with quantum number $n$ [e.g., the one marked $I$ in Fig. 2(b)] correspond to the longest orbits associated with quantum number $n+1$. The deficiencies of the BS approximation are evidently caused by contributions from long orbits. This observation is in line with the well-known failure of the BS approximation to yield the energy gap for chaotic $N$ billiards,[24–26] also caused by long orbits. We also see a discrepancy above the cusp marked $II$ in Fig. 2(b) which turns out to be due to a different source of diffractive scattering at the corner. We will discuss diffractive effects in more detail below when we explore different mechanisms for the failure of the BS approximation by changing the geometry.

### B. Stretched separable billiard

We consider now the separable case $W=D$ but stretch the billiard to $D/L \ll 1$ [see Fig. 4(a)] without, however, changing the Fermi energy $E_F$ of the system. The distance $l$ travelled between two encounters with the SN interface is, for the shortest orbits, at least $2L$. The effect of imperfect retracing, originating from the difference in angles between $\theta_e$ and $\theta_h$, is a divergence between electron and hole trajectories ($\propto l$), which is amplified by large $L$. We introduce as a measure for the imperfect retracing the lateral displacement $\delta y$ on the interface between the hole and the particle trajectory after one loop (see Fig. 5),

$$\delta y = l|\sin(\theta_e) - \sin(\theta_h)| = l\frac{\varepsilon \sin\theta}{E_{\mathrm{F}}} + O(\varepsilon^2), \qquad (12)$$

where $\theta = \theta_{e,h}|_{\varepsilon=0}$. For the particular geometry considered [Fig. 4(a)], $\delta y$ increases linearly with both the trajectory length $l$ and the excitation energy $\varepsilon$. Note that the ratio $\varepsilon/E_{\mathrm{F}}$ is, in general, much smaller than one, i.e., $\varepsilon \leqslant \Delta \ll E_{\mathrm{F}}$.

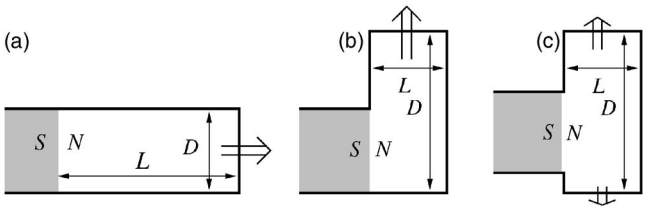


FIG. 4. Geometries with tunable boundaries. (a) Stretched N cavities with $L \gg D$ but with $D$ equal to the width of the SN interface $W=D$. (b) Stretched N cavities with $D \gg L$ but constant length $L$ (lower boundary of S and N aligned). (c) As in (b) but SN interface at arbitrary position on the entrance side.

This classical scale for the mismatch between the particle and hole orbits should be related to the quantum scale, i.e., the linear dimension of the wave packet estimated by the de Broglie wavelength $\lambda_F$. We thus introduce $r=|\delta y|/\lambda_F$ as the order parameter for the error of retracing. For $r \ll 1$ the wave packet cannot resolve the mismatch and the BS approximation should work well. Conversely, as $r$ reaches the order of unity, quantization based on the existence of a continuum of periodic orbits should fail.

To probe the breakdown of the retracing approximation quantitatively, we compare the semiclassical with the quantum density of states (DOS), which are obtained from the state counting function $N(\varepsilon)$ as

$$\rho_{\mathrm{BS,QM}}(\varepsilon) = \frac{\partial N_{\mathrm{BS,QM}}(\varepsilon)}{\partial \varepsilon}, \qquad (13)$$

since the DOS is more sensitive to errors than the (smoothed) spectral staircase. Results for two cavities with different values of $L$ are shown in Figs. 6(a) and 6(b). This example illustrates that the degree of agreement between $\rho_{\mathrm{QM}}$ and $\rho_{\mathrm{BS}}$ is indeed controlled by $r$. The following trends can be observed: ($i$) Due to the comparatively shorter length $l$ of orbits in (a), the overall agreement there is better in (a) than in (b). ($ii$) The agreement in (b) deteriorates for

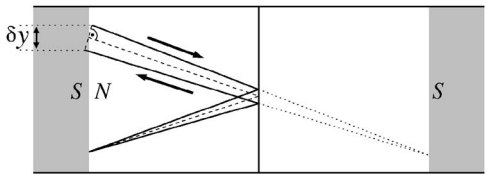


FIG. 5. Imperfect Andreev reflection in the fundamental and extended zone scheme. The returning hole hits the SN interface a distance $\delta y$ apart from the starting point of the particle.

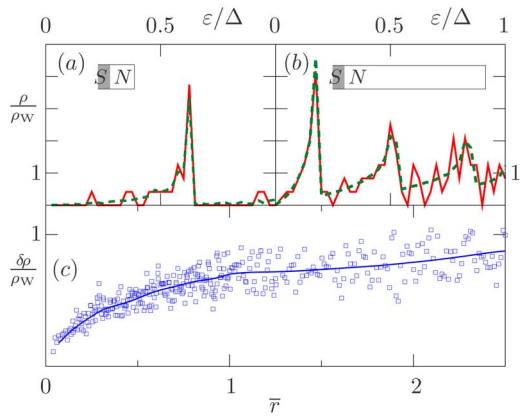


FIG. 6. (Color online) The DOS calculated quantum mechanically (red solid curve) and by the BS approximation (green dashed curve) for two different geometries with ratios of (a) $L/D=1$ and (b) $L/D=6$ (see insets) in units of the Weyl approximation of the DOS per unit area, $\rho_W=m_{\mathrm{eff}}/(\hbar^2\pi)$. (c) Error of the semiclassical prediction $\delta\rho$ [Eq. (15)] as a function of an energy-averaged $\bar{r}$ [Eq. (14)] for 300 different ratios of $L/D\in[1,20]$. The solid blue line shows a smoothed average (30 adjacent points) of the recorded data.

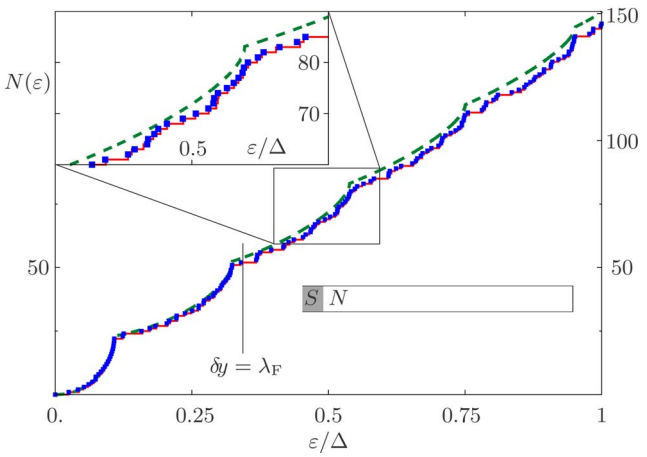


FIG. 7. (Color online) Comparison of the exact quantum mechanical state counting function $N_{\mathrm{QM}}$ (red staircase) with the semiclassical BS (green dashed line) and EBK (blue squares) approximations for a highly elongated cavity ($L/D=10$), as shown in the lower inset. Quantum mechanical and EBK solutions are nearly indistinguishable. The upper inset shows a magnification. The energy for which $\delta y=\lambda_{\mathrm{F}}$ is marked.

larger values of $\varepsilon/\Delta$, since the mismatch in retracing increases with $\varepsilon$.

As a measure for the average mismatch between $\rho_{\mathrm{QM}}$ and $\rho_{\mathrm{BS}}$ in an Andreev billiard of the given geometry we use the quantity $\overline{\delta y}$, which is $\delta y$ averaged over all $\varepsilon$ and all angles,

$$\overline{\delta y}=\frac{1}{\pi\Delta}\int_{-\pi/2}^{\pi/2}d\theta\cos\theta\int_0^{\Delta}d\varepsilon\,\delta y=\frac{2L\Delta}{\pi E_{\mathrm{F}}},\qquad(14)$$

since for this particular geometry $l=2L/\cos\theta$. The error in the DOS is quantified in terms of the root mean square (rms) deviation $\delta\rho$ between $\rho_{\mathrm{BS}}$ and $\rho_{\mathrm{QM}}$,

$$\delta\rho=\sqrt{\frac{1}{\Delta}\int_0^{\Delta}\mathrm{d}\varepsilon|\rho_{\mathrm{QM}}-\rho_{\mathrm{BS}}|^2}.\qquad(15)$$

As expected, as long as $\bar{r}=\overline{\delta y}/\lambda_{\mathrm{F}}\ll 1$, the retracing approximation is sufficiently accurate to reproduce the DOS on the scale of the mean level spacing [see Fig. 6(c)]. Note that resolution of individual levels is beyond the scope of the BS approximation. As discussed below, an EBK quantization is needed for an accurate quantization of individual levels. As $\bar{r}$ approaches unity the oscillations in the quantum DOS cannot be resolved any longer. The error $\delta\rho(\overline{\delta y})$ appears to saturate, in agreement with the observation that in this regime the main peaks in Fig. 6(b) [corresponding to the main cusps in $N(\varepsilon)$] remain well described by the retracing approximation. Identifying the latter with the shortest Andreev-reflected orbits of length $\sim 2L$ allows a simple explanation as to why even a drastic elongation of the cavity leaves these cusps well described by the retracing approximation: orbits of length $\sim 2L$ correspond to strictly horizontally injected trajectories (with $\theta=0$). They do not accumulate any lateral displacement $\delta y$ irrespective of the length of the orbit and $\varepsilon$. While the average value $\overline{\delta y}$ is increasing with growing cavity elongation (due to orbits with $\theta\neq 0$), the horizontal orbits limit the increase $\delta\rho(\overline{\delta y})$, leading to the observed saturation in Fig. 6(c) for $\overline{\delta y}>\lambda_{\mathrm{F}}$.

Additional evidence that the discrepancy between the quantum DOS and the BS spectrum is due to the retracing assumption (A1) and not due to the failure of semiclassics itself (A3) can be gained from an EBK quantization. Note that the Andreev system [Fig. 4(a)] is separable. Moreover, regions in phase space that will not make contact with the SN interface are in this geometry of measure zero, i.e., assumption A2 is valid. In sharp contrast to the discrepancy between $N_{\mathrm{QM}}$ and $N_{\mathrm{BS}}$, we observe that $N_{\mathrm{QM}}$ and $N_{\mathrm{EBK}}$ agree almost perfectly in the whole energy interval $0\leqslant\varepsilon\leqslant\Delta$ (see Fig. 7) even for very elongated cavities where most orbits are non-retracing ($\delta y>\lambda_F$). The criterion $\delta y\approx\lambda_F$ is found to be a good estimate where the BS quantization deviates from both the EBK quantization and the exact quantum spectrum. The case of the elongated N billiard clearly demonstrates that the failure of the BS quantization in this case is due to the retracing assumption (A1), but not due to the failure of semiclassics (A3) itself.

### C. Stretched nonseparable billiard

We focus now on billiards stretched in the direction of the SN interface with $D/W\gg 1$ and $D/L\gg 1$ [Figs. 4(b) and 4(c)]. For $D/W>1$ the Andreev billiard becomes nonseparable and an EBK quantization is no longer rigorously justified. However, as we will show below, the predictions by the BS quantization can still be compared with an approximate EBK quantization. As the wave functions (Fig. 8) clearly indicate, the retracing approximation breaks down with large discrepancies between the particle ($|u|^2$) and hole ($|v|^2$) densities occurring. For this system, one obvious culprit is assumption A2. An extended region of classical phase space (Fig. 9) remains decoupled from the SN interface. Conse-

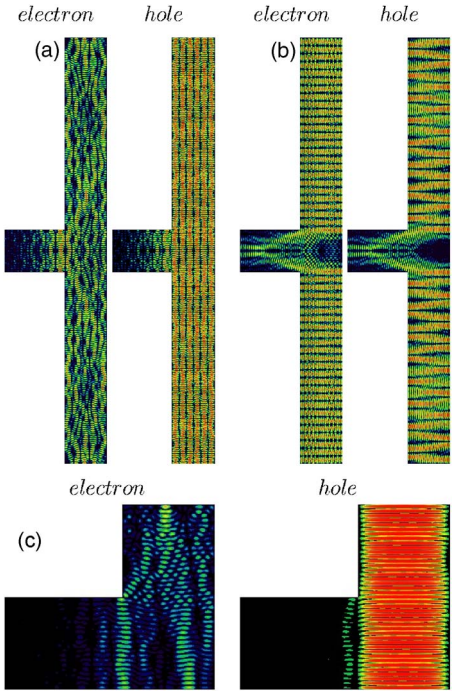


FIG. 8. (Color online) Selected Andreev eigenstates of nonseparable Andreev billiards stretched parallel to the SN interface displaying a large discrepancy between electron and hole wave function patterns. (a) $L/D=10$, $\varepsilon=0.760\Delta$; (b) $L/D=10$, $\varepsilon=0.766\Delta$, $k_F=21.5\pi/W$; and (c) $L/D=2$, $\varepsilon=0.040\Delta$, $k_F=20.5\pi/W$;

quently, the quantum DOS is associated, in part, with decoupled regions which are not represented at all by the BS approximation. It has previously been pointed out for other geometries (whispering gallery trajectories in circular billiards) that Andreev billiards indeed feature quantum states that are not associated with periodic electron-hole orbits.[15]

A more detailed inspection reveals that a certain class of wave functions has the following features: (1) The probability density at the SN interface is typically low—corresponding to decoupling from the superconductor. This suggests that the SN interface effectively acts like a hard-wall boundary. (2) Integrating the probability density in the electron- and hole-part of the N region typically shows a strong asymmetry. For the case depicted in Fig. 8(c) we calculate a probability of 98.3% for the hole component and only 1.3% for the particle component. The coupling with the superconductor is very weak, resulting in a probability of 0.4% of finding the particle in the superconducting lead. These observations suggest that the particles in such nonretracing states are quasibound in either the electron- or the hole-space with only infrequent and short excursions to their respective mirror space. As a consequence we may employ again an EBK quantization scheme to estimate the corresponding energy level of the Andreev state, however now in the space of the quasi-bound particle or hole. Exploiting the assumption of weak coupling to the SN interface, we replace the SN interface by a hard-wall (box) boundary. Applying this approach, e.g., to the state depicted in Fig. 8(a), the EBK quantization

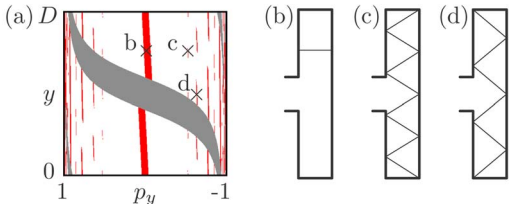


FIG. 9. (Color online) (a) Poincaré surface of section of a stretched nonseparable Andreev billiard, taken at the right vertical side, opposing the SN interface: $W/D=5$, $W=L$. The light gray area marks regions of classical phase space coupled directly to the entrance lead, with one single reflection at the right wall. Dark red areas show regions of classical phase space decoupled from the superconducting lead. Classical trajectories corresponding to selected areas of phase space are marked by crosses in (a) and shown in (b)–(d).

$$E_{n,m}=\frac{1}{2}\left(\frac{n\pi}{L}\right)^2+\frac{1}{2}\left(\frac{m\pi}{D}\right)^2 \tag{16}$$

implies for the density of the "isolated" electron state $n=6$ maxima in the $x$ direction and $m=205$ maxima in the $y$ direction. Inserting these quantum numbers yields an excitation energy of $\varepsilon_{\mathrm{box}}=0.753\Delta$, which is very close to the exact eigenenergy of the Andreev eigenstate of $\varepsilon_{\mathrm{QM}}=0.760\Delta$. Analogously, the state depicted in Fig. 8(c) has quantum numbers $n=1$, $m=41$, corresponding to a hole excitation of $\varepsilon_{\mathrm{box}}=0.038\Delta$, which compares well to the eigenenergy of the Andreev eigenstate of $\varepsilon_{\mathrm{QM}}=0.040\Delta$. While the position of these Andreev states can thus be explained fairly accurately by a box (or EBK) quantization, they are obviously not included in a standard BS approximation which considers only retracing electron-hole orbits. This illustrates the failure of assumption A2, while semiclassics still remains applicable.

### D. Diffractive effects

For the present hard-wall N cavities, introducing nonseparability implies simultaneously the introduction of diffractive edges and corners (see Fig. 4).[36] In the preceding example, diffractive effects were present but for the special group of states considered of minor importance. The latter was confirmed not only by the density distributions in the Andreev states (Fig. 8) but also by the accuracy of the EBK prediction. We can now enhance diffractive effects by considering only moderately stretched cavities $D/W>1$ with arbitrary position of the SN interface. As shown in Fig. 10, we can thus realize Andreev billiards with zero corners ($D/W=1$), one corner ($D/W>1$, lower boundary of S and N aligned), and two corners ($D/W>1$, arbitrary position of the SN interface). Diffractive effects originate from potential variations on a length scale smaller than the de Broglie wavelength. In a semiclassical picture, diffractive scattering gives rise to a nondeterministic, stochastic angular distribution. It certainly prevents the deterministic perfect retracing of orbits.

Diffractive scattering can be directly visualized in the wave function [Figs. 10(b) and 10(c)]. The density enhance-

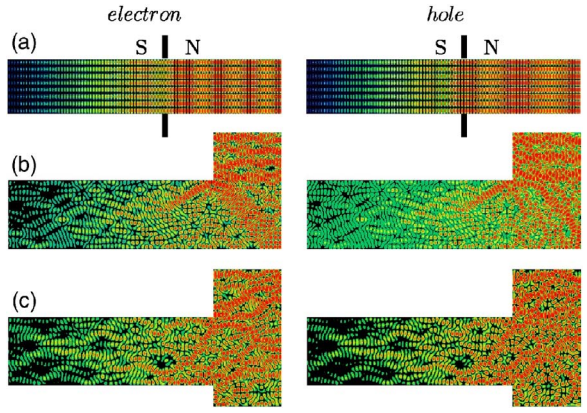


FIG. 10. (Color online) Selected Andreev eigenstates of systems with (a) no diffractive corners ($L/D=1.6$, $W=D$, $k_F=20.5\pi/W$, $\varepsilon/\Delta=0.48$); (b) one diffractive corner ($D/L=1.7$, $W=L$, $k_F=21.5\pi/W$, $\varepsilon/\Delta=0.72$); and (c) two diffractive corners ($D/L=1.7$, $W=L$, $k_F=20.5\pi/W$, $\varepsilon/\Delta=0.82$).

ment representing a scar of a classical trajectory hits the corner of the SN interface. As a result the trajectory "splits" into a bouncing-ball orbit and a broad angular distribution. Significant differences between the particle ($|u|^2$) and hole ($|v|^2$) density in the retracing orbit are clearly visible.

For a more quantitative assessment we compare again the quantum and the BS results for the DOS [see Figs. 11(a) and 11(b)] and find, similarly to the case of the separable geometry, that for larger $D$ the mismatch $\delta\rho$ in the DOS increases. If we compare, however, how the error $\delta\rho$ scales with the geometric retracing mismatch $\delta y$ [Fig. 11(c)], we find that in the Andreev billiard with a diffractive corner the average mismatch is considerably larger than for the geometry without a sharp corner. The difference in $\delta\rho$ at fixed $\overline{\delta y}$ can be thus attributed to diffraction. Note that diffractive scattering

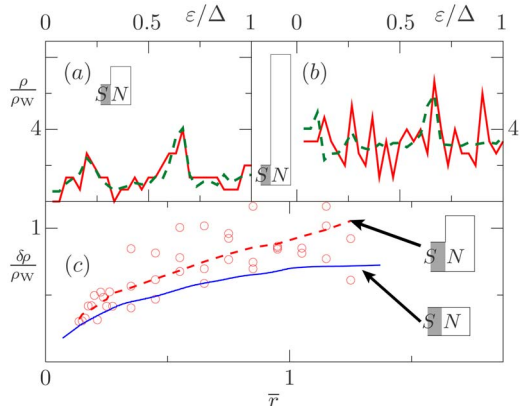


FIG. 11. (Color online) The DOS calculated quantum mechanically (red solid curve) and by the BS approximation (green dashed curve) for two different geometries with ratios of (a) $L/D=1$ and (b) $1/8$ (see insets), in units of the Weyl approximation of the DOS per unit area, $\rho_W=m_{\text{eff}}/(\hbar^2\pi)$. (c) Error of the retracing approximation $\delta\rho$ [Eq. (15)] for transversely elongated cavities (red circles) as a function of $\bar{r}$. The solid blue (dashed red) line shows the average error for longitudinally (transversely) elongated cavities (see also Fig. 6).

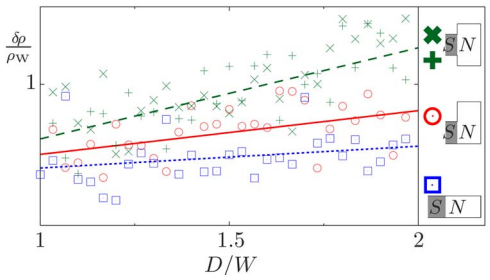


FIG. 12. (Color online) Error of the retracing approximation $\delta\rho$ as a function of $D/W$ for geometries with no (blue square, dashed line), one (red circle, solid line), and two (green cross, dashed line) diffractive corners. Different orientations of the cross refer to different positions of the superconducting lead. The lines show a linear root mean square fit to the data.

is an additional mechanism for the failure of the retracing approximation, which is independent of the failure induced by long electron-hole orbits.

Additional evidence along these lines is presented in Fig. 12 where the mismatch $\delta\rho$ between the BS approximation and the quantum results as a function of the geometrical aspect ratio of the normal-conducting region is compared for three geometries with either (a) zero, (b) one, or (c) two diffractive corners at the SN interface. As expected, the mismatch increases (1) for larger aspect ratios and (2) at fixed aspect ratio for an increasing number of diffractive corners. Further support comes from the observation that the mismatch $\delta\rho$ for the cavity with two diffractive corners is, to a large degree, independent of the position of the lead, as shown in Fig. 12.

Unlike other sources for the failure of the retracing approximation discussed above, diffraction limits the validity of standard semiclassical approximations itself, i.e., the validity of assumption A3. Methods for describing diffractive effects semiclassically by including pseudopaths[37,38] and nondeterministic scattering[39] have been explored for scattering at open N cavities. They play a crucial role in determining the S matrix for such devices. The present results demonstrate that diffractive corrections come into play also for Andreev systems.

## IV. CONCLUSION

We study Andreev billiards of rectangular shape and compare the quantum solutions of the Bogoliubov-de Gennes equation with a semiclassical Bohr-Sommerfeld approximation that assumes retracing electron-hole orbits as a result of perfect Andreev reflection. Investigating the validity of this widely used semiclassical approach, we identify three independent mechanisms which influence the density of bound Andreev states beyond the simple BS quantization: (*i*) long trajectories in the billiard typically magnify deviations between the electron and the hole part of orbits and cause a failure of the retracing approximation. This is of importance for the understanding of the failure of the BS approximation to reproduce the hard gap for chaotic N cavities. The latter is

controlled by the behavior of long paths for which, as we show, the retracing approximation breaks down. (*ii*) BS quantization fails when a subspace of the phase space is decoupled from the SN interface and thus is inaccessible to retracing orbits. (*iii*) Diffractive effects limit the validity of the semiclassical quantization. In the latter case the failure is not just due to the assumption of retracing, but due to the failure of standard semiclassics itself. In this case, also alternative methods such as EBK quantization of separable or adiabatic quantization[33,34] of (smooth) chaotic systems will fail. Corrections beyond standard semiclassics, e.g., inclusion of pseudo-paths[37,38] of diffracted orbits, will be needed.

## ACKNOWLEDGMENTS

We thank F. Aigner, J. Cserti, B. L. Györffy, A. Kormányos, and C. J. Lambert for valuable discussions. Support by the Austrian Science Foundation (Grant No. FWF-P17359), the Hungarian-Austrian Intergovermental S&T cooperation program (Project No. 2/2003), and the British Council Vienna is gratefully acknowledged.

*Electronic address: florian@concord.itp.tuwien.ac.at

[1] A. F. Morpurgo, S. Holl, B. J. van Wees, T. M. Klapwijk, and G. Borghs, Phys. Rev. Lett. **78**, 2636 (1997).
[2] H. Pothier, S. Guéron, D. Esteve, and M. H. Devoret, Phys. Rev. Lett. **73**, 2488 (1994).
[3] P. Charlat, H. Courtois, P. Gandit, D. Mailly, A. F. Volkov, and B. Pannetier, Phys. Rev. Lett. **77**, 4950 (1996).
[4] C. J. Lambert and R. Raimondi, J. Phys.: Condens. Matter **10**, 901 (1998).
[5] P. F. Bagwell, Phys. Rev. B **46**, 12573 (1992).
[6] M. Stone, Phys. Rev. B **54**, 13222 (1996).
[7] C. W. J. Beenakker, Rev. Mod. Phys. **69**, 731 (1997).
[8] I. Kosztin, D. L. Maslov, and P. M. Goldbart, Phys. Rev. Lett. **75**, 1735 (1995).
[9] J. Wiersig, Phys. Rev. E **65**, 036221 (2002).
[10] K. P. Duncan and B. L. Györffy, Ann. Phys. **298**, 273 (2002).
[11] N. A. Mortensen, K. Flensberg, and A. P. Jauho, Phys. Rev. B **59**, 10176 (1999).
[12] J. Cserti, G. Vattay, J. Koltai, F. Taddei, and C. J. Lambert, Phys. Rev. Lett. **85**, 3704 (2000).
[13] G. E. Blonder, M. Tinkham, and T. M. Klapwijk, Phys. Rev. B **25**, 4515 (1982).
[14] A. Andreev, Sov. Phys. JETP **19**, 1228 (1964).
[15] J. Cserti, A. Bodor, J. Koltai, and G. Vattay, Phys. Rev. B **66**, 064528 (2002).
[16] W. Ihra, M. Leadbeater, J. Vega, and K. Richter, Eur. Phys. J. B **21**, 425 (2001).
[17] J. Cserti, P. Pollner, A. Kormányos, B. Bèri, and Z. Kaufmann, J. Phys.: Condens. Matter **16**, 1 (2004).
[18] S. Gnutzmann, B. Seif, F. von Oppen, and M. R. Zirnbauer, Phys. Rev. E **67**, 046225 (2003).
[19] P. Gennes, *Superconductivity of Metals and Alloys* (Benjamin, New York, 1966).
[20] H. Schomerus and C. W. J. Beenakker, Phys. Rev. Lett. **82**, 2951 (1999).
[21] A. Altland and M. R. Zirnbauer, Phys. Rev. Lett. **76**, 3420 (1996).
[22] A. Kormányos, Z. Kaufmann, J. Cserti, and C. J. Lambert, Phys. Rev. B **67**, 172506 (2003).
[23] F. Libisch, S. Rotter, J. Burgdörfer, A. Kormányos, and J. Cserti, Phys. Rev. B **72**, 075304 (2005).
[24] J. A. Melsen, P. W. Brouwer, K. M. Frahm, and C. W. J. Beenakker, Europhys. Lett. **35**, 7 (1996).
[25] M. G. Vavilov and A. I. Larkin, Phys. Rev. B **67**, 115335 (2003).
[26] D. Taras-Semchuk and A. Altland, Phys. Rev. B **64**, 014512 (2001).
[27] F. Libisch, Master's project, Vienna University of Technology, Institute for Theoretical Physics 2004.
[28] S. Rotter, J.-Z. Tang, L. Wirtz, J. Trost, and J. Burgdörfer, Phys. Rev. B **62**, 1950 (2000).
[29] S. Rotter, B. Weingartner, N. Rohringer, and J. Burgdörfer, Phys. Rev. B **68**, 165302 (2003).
[30] P.-G. de Gennes and D. Saint-James, Phys. Lett. **4**, 151 (1963).
[31] M. Brack and R. Bhaduri, *Semiclassical Physics* (Addison Wesley Publishing Company, Reading, MA, 1997).
[32] F. Libisch, S. Rotter, and J. Burgdörfer, unpublished.
[33] P. G. Silvestrov, M. C. Goorden, and C. W. J. Beenakker, Phys. Rev. Lett. **90**, 116801 (2003).
[34] M. C. Goorden, P. Jacquod, and C. W. J. Beenakker, Phys. Rev. B **72**, 064526 (2005).
[35] L. Wirtz, J.-Z. Tang, and J. Burgdörfer, Phys. Rev. B **56**, 7589 (1997).
[36] J. Wiersig, Phys. Rev. E **65**, 046217 (2002).
[37] L. Wirtz, C. Stampfer, S. Rotter, and J. Burgdörfer, Phys. Rev. E **67**, 016206 (2003).
[38] C. Stampfer, S. Rotter, J. Burgdörfer, and L. Wirtz, Phys. Rev. E **72**, 036223 (2005).
[39] F. Aigner, S. Rotter, and J. Burgdörfer, Phys. Rev. Lett. **94**, 216801 (2005).